World Conference on Timber Engineering Oslo 2023

EXPERIMENTAL AND NUMERICAL INVESTIGATION OF CROSS-LAMINATED TIMBER JOINTS WITH MULTIPLE GLUED-IN RODS

Younes Shirmohammadli[1], Ashkan Hashemi[2], Reza Masoudnia[3], Pierre Quenneville[4]

ABSTRACT: Glued-in rod connections are highly efficient joints in timber structures, with many advantages, including high strength and stiffness, good fire performance, and architectural design advantages. They have been used for many years, mainly for glulam members and, to a limited degree for laminated veneer lumber (LVL) members in new timber structures or reinforcing existing timber buildings. This research covers glued-in rods in Cross-Laminated Timber (CLT) panels to address the growing interest in constructing mid-to high-rise buildings, where hybrid structural systems are frequently used. Therefore, a combined experimental and numerical investigation has been designed to apply such connections in CLT, and full-scale monotonic and cyclic tests have been performed. For the experimental tests, the specimens vary in embedment length and the location of the rods. Moreover, numerical simulations and parametric studies of glued-in rod connections in CLT have been performed to further extend the scope of the study and make conclusions. The simulations are based on a 3D finite element analysis, using a cohesive surface model for the interaction between the epoxy adhesives and the inner surface of the holes. The parametric studies investigated the influence of the anchorage length, the rod diameter, and the rod-to-grain angle on the load-bearing capacity and stiffness of the glued-in rod connections in CLT. The results of this study demonstrates a high potential of these connections in CLT construction with savings on space and cost when compared to conventional timber connections.

KEYWORDS: Glued-in rods, Timber connections, Cross Laminated Timber, Timber Engineering, Numerical Modeling.

1 INTRODUCTION

In timber structures, connections can take up to 70% of the design effort, and the capacity of the structures is generally governed by the strength and stiffness of the connections and joints [1]. Glued-in rods are high-capacity hybrid connections that are largely used for new timber structures and reinforcement of existing timber buildings. They present high strength and stiffness, good resistance against corrosion and fire, present ductile performance, and provide aesthetic benefits [2]. The efficient design and construction of such high-strength connections often determine the level of success of timber structures compared to concrete and steel.

Glued-in rods have been used in New Zealand and other countries for over thirty years for glulam and LVL members, and well-designed timber structures with appropriate materials have shown good structural performance [3]. With the advent of CLT construction, glued-in rod connections demonstrated the potential to be widely implemented. Because the arrangement of layers and manufacturing process of CLT is different from other engineered wood products, the stress distribution and strength of connections in these products can also be different, which requires more detailed studies [4]. Moreover, depending on the CLT member size and structural design, the rods need to be located on the parallel, perpendicular, or on the boundary of two cross-wised layers.

Most of the studies regarding glued-in rods are focused on the single rod investigation, while in real applications, glued-in rods are used in groups. Plastic deformation of connections is frequently used in timber constructions to achieve ductility. Therefore, the behaviour of those crucial connections in terms of ductility and energy dissipation under cyclic loads must be thoroughly understood.

This research looks into monotonic loading and numerical modeling of glued-in rods embedded in various configurations on the edge of CLT panels. Moreover, the cyclic loading performance of glued-in rods is also investigated. The results of the cyclic loading will illustrate the effect of loading on the stiffness and strength of glued-in rod connections to be designed for high seismic regions.

2 Materials and Methods

CLT panels made of New Zealand-grown Radiata pine bonded with one-component polyurethane adhesive were used as the timber part of the connection. The CLT panels consisted of MSG8-grade laminations for longitudinal

[1] Younes Shirmohammadli, The University of Auckland, New Zealand, yshi829@aucklanduni.ac.nz
[2] Ashkan Hashemi, The University of Auckland, New Zealand, a.hashemi@auckland.ac.nz
[3] Reza Masoudnia, University of Waikato, New Zealand, rm667@students.waikato.ac.nz
[4] Pierre Quenneville, The University of Auckland, New Zealand, p.quenneville@auckland.ac.nz

https://doi.org/10.52202/069179-0189

layers and MSG6-grade laminations for transverse layers. In the experimental tests, for CLT specimens with rods embedded perpendicular to the lamination and rods on the boundary of two cross-wised layers, 5-layer CLT panels were used, while for the rods embedded parallel to the grain, 7-layer CLT panels were used, so the outer layers of the CLT specimens were lengthwise for all of the specimens. The panels were cut into specimens with 240 mm width to provide a 3.5*d* edge distance and a 3*d* rod distance. Four M24 threaded rods (8.8 grade) were placed in holes with 30 mm diameter in the parallel, perpendicular, and on the boundary of two cross-wised layers of the CLT panels at two different embedment lengths (250 and 350mm). The dimensions of the CLT specimens holding the glued-in rods are shown in Figure 1.

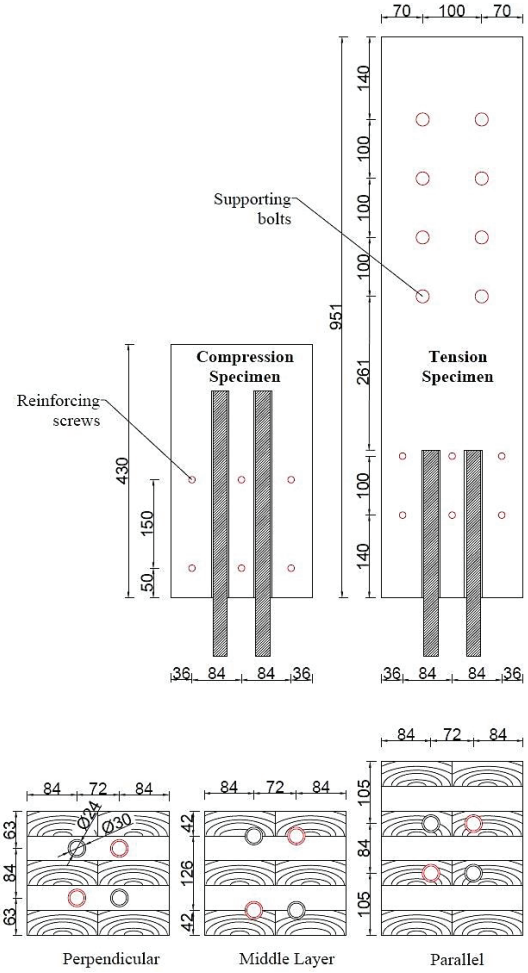

Figure 1. Dimensions of CLT specimens containing rods on the cross section. Rods drawn in red on the cross sections represent two diagonally tested rods.

The epoxy adhesive was injected into the bleeding holes located along each rod's length on the surface of CLT. The adhesive injected from one end of the rod's length travelled the length of the rod and exited from the other end after filling the gap by preventing the air bubble trap. The properties of the applied epoxy adhesive are provided in Table 1.

Table 1. Typical properties of the cured epoxy adhesive.

	Typical cured properties			
Adhesive	Tensile strength (MPa)	Compressive strength (MPa)	Flexural strength (MPa)	Maximum operating temp (°C)
Epoxy	200-300	300-400	350-450	65-75

2.1 Experimental Tests

For the monotonic and cyclic tests, two diagonal rods were tested. The specimens containing rods with 250 mm embedment length were tested in tension, while specimens with 350 mm embedment length were tested in compression for both monotonic and cyclic tests. The 1000 kN Avery machine at the University of Auckland test hall was used for the monotonic loading, and a 500 kN MTS was used for the cyclic loading of the glued-in rod connections. The test setup of the cyclic tests is shown in Figure 2.

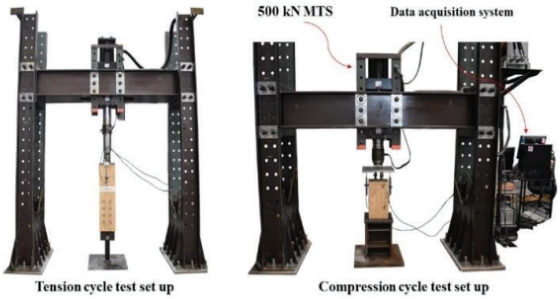

Figure 2. Cyclic loading test set-up.

For the tension tests, the CLT specimens were fixed using two knife plates inserted into the pre-cut slots in the transverse layers of CLT and held by eight M20 bolts. At the other end, a pulling steel member was designed and used to pull out two diagonal glued-in rods at the same time. Figure 3 shows the components of the CLT specimen with rods embedded perpendicular to the lamination to be tested in tension. The monotonic loading was applied at a constant displacement rate of 2 mm/min throughout the loading process. The average displacement/slip of the rods was measured using two LVDTs.

https://doi.org/10.52202/069179-0189

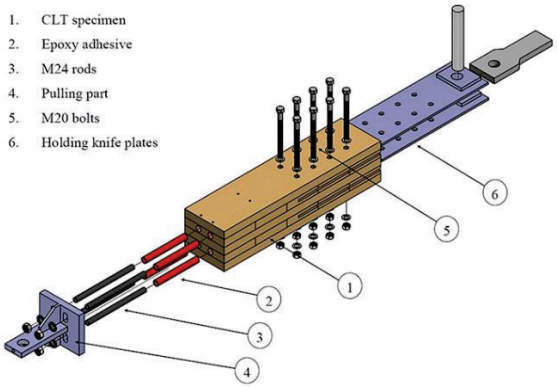

Figure 3. Exploded view of 5-layer CLT specimen with rods embedded perpendicular to the grain.

A loading procedure from BS EN 12512:2001 [7] was modified for cyclic loading. Due to the stiffness of the glued-in rod connections with failure occurring within 1-2 mm displacement of the rods, the rods were loaded in a force-control manner at a rate of 5 kN/s. The force reference for the cyclic loading was determined from the monotonic loading. For testing under cyclic loads, CLT specimens with 250 mm embedded length rods were subjected to tension-only cycles, while specimens with 350 mm embedment length rods were subjected to compression-only cycles. The specimens were put through a tension/compression load in the first cycle that applied 25% of the maximum load. Then, the load was released until zero force. The initial cycle was repeated in the second cycle, but this time 50% of the force was applied. In the third round, three cycles are completed at 75% of the maximum load. For the CLT specimens containing rods with 250 mm embedment length, the load was then increased until failure occurred, and for the specimens containing rods with 350 mm embedment length, three more cycles at the maximum load were established. Glued-in rods with embedment lengths of 250 mm were tested until they failed on the last cycle. However, specimens with embedment length of 350 mm did not fail within the standard range by the machine capacity. The loading cycles of specimens with 250 and 350 mm embedment lengths are shown in Figure 4.

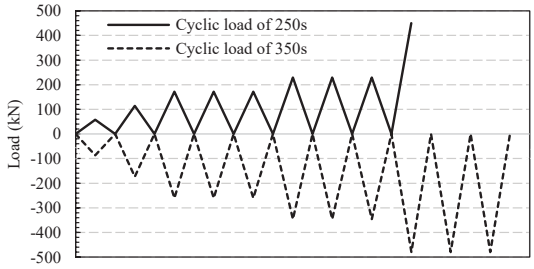

Figure 4. Cyclic loading protocols.

2.2 Numerical Modeling

The numerical analysis is performed using the Abaqus software package (finite element analysis software) [8] to investigate the effect of the rod diameter and embedment length on the pull-out strength and to study the stress distribution along the rods. The 3D model of the CLT panel was designed with cross-wised laminations with orthotropic properties (E_1= 10400 MPa, E_2-E_3= 347 MPa, ν_{12}= ν_{13}= ν_{23}= 0.2, G_{12}=G_{13}= 692, and G_{23}= 69) and tied interaction between the laminations and no edge bonding as in the tested CLT panel. While the properties of the rods (E=210000 MPa and ν=0.3) and epoxy adhesive (E= 2193 MPa and ν= 0.3) were defined as an isotropic material. The interaction between the rod's surface and the inner surface of the epoxy adhesive is defined as a 'tie' since in the experimental tests, no failure was observed (due to the excellent interaction of the threads of the rods and epoxy adhesive). The experimental test data was used to validate the numerical models. The load was applied to the rods with a displacement-based approach, and a rigid body was defined at the end of the CLT specimen and fixed as a boundary condition in the Z-direction to measure the reaction force. The numerical model of the glued-in rod connection is shown in Figure 5.

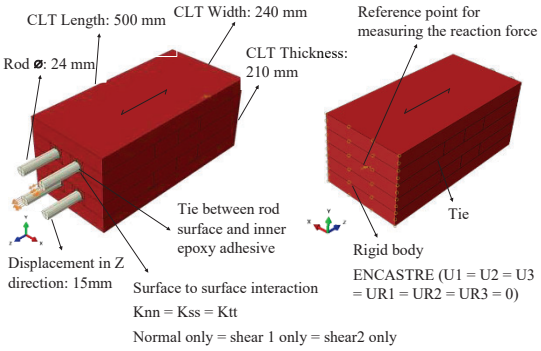

Figure 5. FE modeling of the glued-in rods connection with rods located on the perpendicular layers of CLT.

For each rod to grain configuration, different interaction properties are defined between the outer surface of the epoxy adhesive and the inner surface of the hole, which are shown in Table 2.

Table 2. Interaction properties of embedded rods regarding the rod to lamination angle.

Rod to grain orientation	*Knn* (N/mm^3)	*Kss* (N/mm^3)	*Ktt* (N/mm^3)	*Normal (MPa)*	*Shear-1 (MPa)*	*Shear-2 (MPa)*
Parallel	160	160	160	14.2	14.2	14.2
Perpendicular	225	225	225	14.5	14.5	14.5
Boundary	320	320	320	14.7	14.7	14.7

3 RESULTS AND DISCUSSIONS

3.1 Experimental tests

3.1.1 Monotonic loading

The average pull-out strength of glued-in rods with 250 mm embedment length is shown in Figure 6. For the rods embedded on the perpendicular, parallel, and boundary of

https://doi.org/10.52202/069179-0189

two cross-wised layers, the average pull-out strength of glued-in rods with 250 mm embedment length was 343 kN, 333 kN, and 305 kN, respectively. The shorter distance between the rods and the CLT surface led to a lower pull-out strength of the rods embedded on the boundary of two cross-wised layers. As a result, the stress reached the surface of the CLT specimen and formed a premature crack, subsequently leading to a lower pull-out strength. The glued-in rods with 350 mm embedment length at the perpendicular, parallel, and boundary of two cross-wised layers had average compression strengths of 506, 493, and 482 kN, respectively. The connection strength also decreased as a result of the lower surface distance of the rods embedded on the boundary of two cross-wised layers. The average compression strength of rods with 350 mm of embedment is displayed in Figure 6.

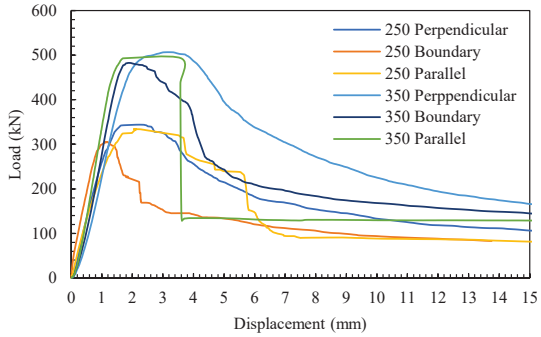

Figure 6. Average values for strength of glued-in rods with 250 and 350 mm embedment length.

The yielding of the steel rods in glued-in rod connections is intended to produce a ductile failure mode. To obtain the tolerance threshold of brittle failure and other types of failures of the connection components, this research was set up so that the steel rods' strength was greater than that of the other connection components. Given the characteristics of CLT, the specimen's failure mode can be influenced by its specifications, including laminations dimension, laminations grade, bonding, etc. For instance, not edge-bonded laminations, weak finger joints, and knots can initiate the failure and reduce the strength of the connection. Common failure modes of CLT specimens with rods embedment at the edge of CLT is shown in Figure 7.

Various potential failures have been reported in the literature for rods embedded perpendicular to the lamination. Most common failure types for rods implanted perpendicular to the grain is the separation of the entire transverse layer or rolling shear [5, 6]. Rolling shear failure in the transverse layers was the observed mode of failure for the rods embedded perpendicular to the lamination, as illustrated in Figure 7a. This is due to the lower tangential and radial strength of the wood. When glued-in rods are used as a connection, the failure in thetransverse layer caused by rolling shear revealed the need for reinforcing the CLT. Rolling shear still seems inevitable despite increasing the edge distance, and it is unaffected by the geometrical characteristics of the connection. This progressive rolling shear failure resulted in a smooth force-displacement curve. However, when the rods were put perpendicular to the grain, the stress did not reach the surface of the CLT. The epoxy adhesive was also crushed along the length of the rods.

The parallel to the grain rods were pulled out in the shape of plugs that held parallel lamination segments, as seen in Figure 7b. Therefore, whether it happened close to the wood-adhesive contact or by removing a block of wood, block shear of wood caused the connections to fail and resulted in a sharp strength reduction. The surface and edge of CLT specimens for the rods embedded parallel to the grain showed no signs of damage. The amount of plugged-out wood close to the rods could potentially be impacted by the non-edge bonded laminations. Similar plug-out failures have been recorded for rods inserted parallel to the lamination in the literature [9].

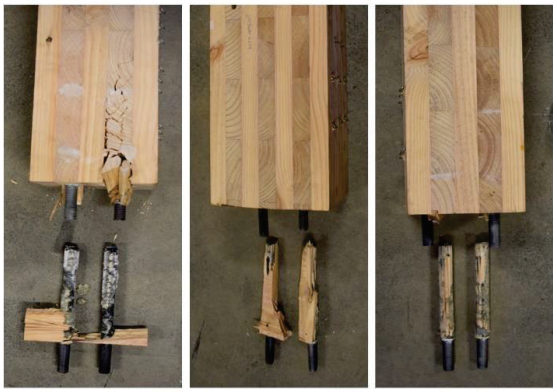

Figure 7. Failure modes on the edge of CLT specimens under tension test, (a) rods perpendicular to the lamination, (b) rods parallel to the lamination, and (c) rods embedded on the boundary of two cross-wised layers.

Rods inserted in the boundary of two cross-wised layers were entirely pulled out in the shape of a cylinder gripping the epoxy that had wood fibres on its surface, as shown in Figure 7c. Moreover, Figure 8 illustrates the influence of the rod's close proximity to the CLT surface by showing the failure mode of rods embedded on the boundary of two cross-wised layers while stress reaching the specimen's surfaces for both tension and compression specimens. When two lengthwise laminations that are not edge-bonded are situated close to the rod's length, this issue gets worse. Regarding the crack spreading to the CLT's surface, the edges of the specimens revealed no signs of damage. This crack formation has also been noticed in glulam specimens with glued-in rods due to the close edge distance, reaching the specimens' surface along the embedment length [10].

https://doi.org/10.52202/069179-0189

Figure 8. Surface crack of specimens containing rods on the boundary of two cross-wised layers.

3.1.2 Cyclic loading

Figure 9 provides an overview of the hysteresis response of the cyclic tests conducted on the glued-in rods embedded in CLT. All curves for the specimens with a 250 mm embedment length displayed a nearly linear trend at cycles until failure. Glued-in rods with 250 mm embedment length that were located perpendicular, parallel, and on the boundary of two cross-wised layers failed at 331, 317, and 297 kN, respectively. The connections for the rods with 350 mm embedment length demonstrated stiff and elastic performance, but there was a slight plastic deformation at each cycle in the last three cycles of the tests.

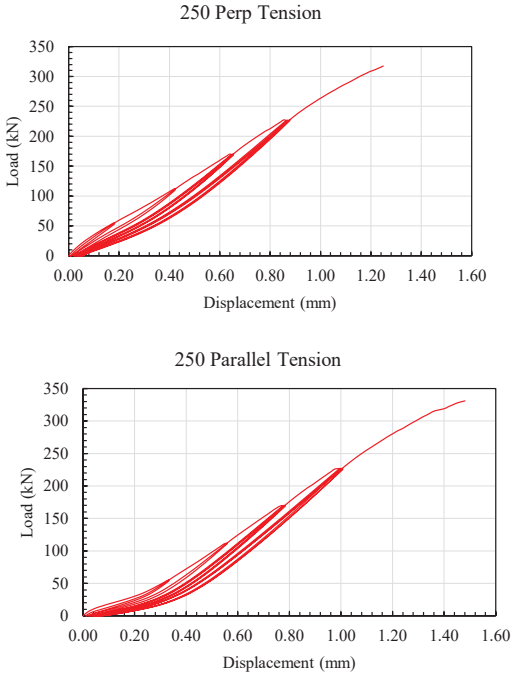

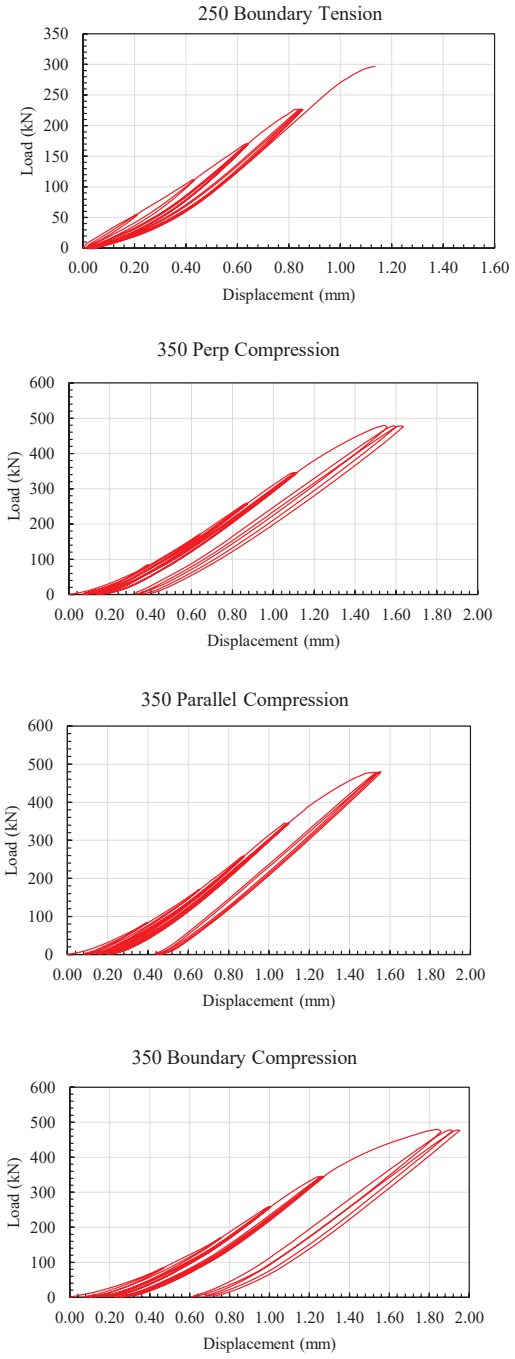

Figure 9. Hysteresis loops of glued-in rods under cyclic loading.

In contrast to glued-in rods with 250 mm embedment length, specimens with 350 mm anchorage length did not fail during the final cyclic tests. The specimens with 250 mm embedment length showed failure modes similar to monotonic tests.

https://doi.org/10.52202/069179-0189

3.2 Numerical modeling

3.2.1 Numerical modeling validation

Experimental tests were used to validate the numerical models. For every embedded rod that was parallel, perpendicular, or in the boundary of two cross-wised layers, high-precision validations were prepared. Maximum failure load, connections stiffness, and failure mode were the three characteristics used to evaluate the accuracy of the numerical modeling validations.

Table 3 compares the maximum loads of numerical models with the outcomes of experimental tests. The numerical models of rods with 250 mm embedment length at different locations were able to predict the pull-out strength with an average of 2% difference.

When the numerical models had been validated for rods with an embedment length of 250 mm, the prediction accuracy of the models was evaluated using experimental test results for rods with an embedment length of 350 mm. For the rods with 350 mm length which were modelled in tension, the numerical models estimated the pull-out strength of the rods with an average of 4% difference. The numerical models predicted the strength of glued-in rods with an overall P_{Test}/P_{FE} of 0.992 and a standard deviation of 0.028, as shown in Table 3. The higher discrepancy between the numerical modeling and experimental tests of rods with 350 mm embedment length was because rods were tested experimentally in compression while they were analysed in tension for the numerical modeling.

Table 3 Comparison of maximum strength of rods between experimental tests (P_{TEST}) and numerical modeling (P_{FE})

Rod to grain orientation	Embedment length (mm)	P_{Test}	P_{FE}	P_{Test}/P_{FE}
	L_a	(kN)	(kN)	
Perpendicular	250	344.0	346.7	0.99
Perpendicular	350	506.6	525.8	0.96
Boundary	250	305.2	310.0	0.98
Boundary	350	482.5	464.1	1.04
Parallel	250	333.9	331.8	1.01
Parallel	350	493.0	510.3	0.97
Average				0.992
Standard Deviation				0.028

The stiffness of the connections was also used to validate the numerical models. Figure 10 exhibits the strong conformity in stiffness between the numerical simulation and experimental tests of the M24 rods embedded perpendicular to the lamination of CLT and the experimental tests. Regarding the specified interaction properties in the numerical models, after following the stiffness and reaching the maximum load, it loses strength, although for the experimental tests, a gradual force reduction was obtained.

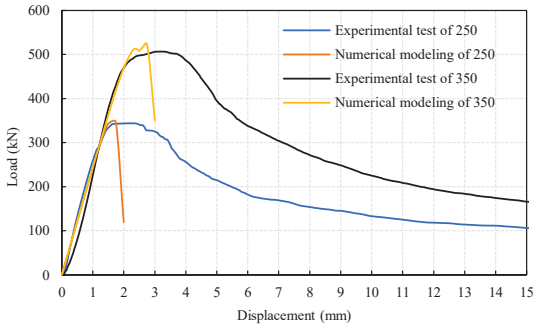

Figure 10. The force vs. displacement curves of numerical modeling and experimental tests for rods with 24 mm diameter and 250 mm anchorage length embedded perpendicular to the lamination.

In the experimental tests of rods embedded on the boundary of two-cross-wised layers, a crack appeared along the length of the rods on the surface of the CLT specimens. The numerical modeling of rods embedded on the boundary of two cross-wised layers revealed the same stress distribution that reached the surface of the CLT specimens, as shown in Figure 11.

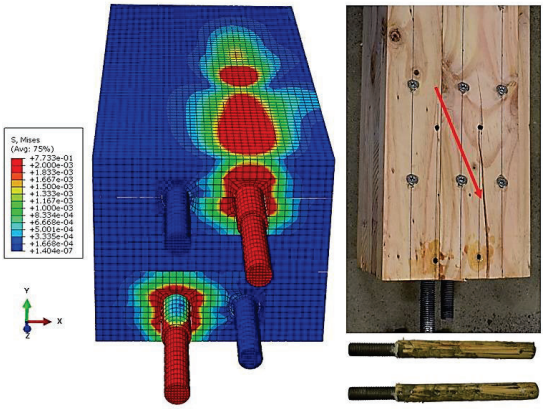

Figure 11. Numerical modeling and experimentally tested specimens of rods embedded on the boundary of two cross-wised layers.

Moreover, experimental tests of the rods embedded perpendicular to the lamination demonstrated rolling shear failure in the transverse layers. The stress distribution and displacement indicated by the numerical modeling of rods embedded perpendicular to the grain were predicted to reach the edge of the CLT specimen and cause rolling shear, as illustrated in Figure 12.

https://doi.org/10.52202/069179-0189

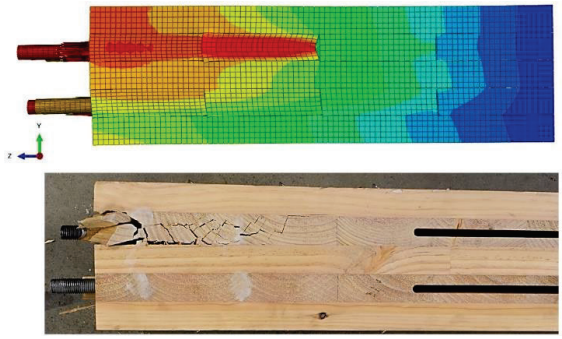

Figure 12. Numerical modeling and experimentally tested specimens of rods embedded perpendicular to the laminations.

3.2.2 Parametric investigation

The parametric study of two rods embedded perpendicular to the laminations and tested diagonally revealed that the pull-out strength increased with increasing the rod diameter and embedment length, as shown in Figure 13. Two rods with 30 mm diameter and embedment lengths of 450 mm reached a pull-out strength of 961 kN.

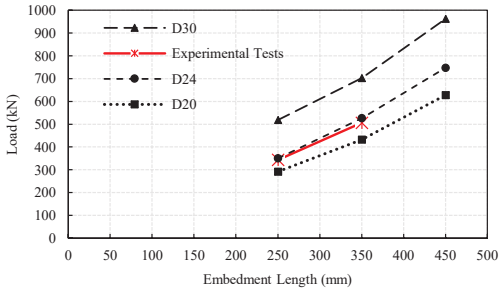

Figure 13. Numerical modeling and experimental test results of rods embedded perpendicular to the grain.

The pull-out strength of the numerical model of the two diagonal rods embedded parallel to the grain increased as the rod diameter, and embedment length increased. The pull-out strength of the rods reached 836 kN for two rods with 30 mm diameter and an embedment length of 450 mm, as shown in Figure 14.

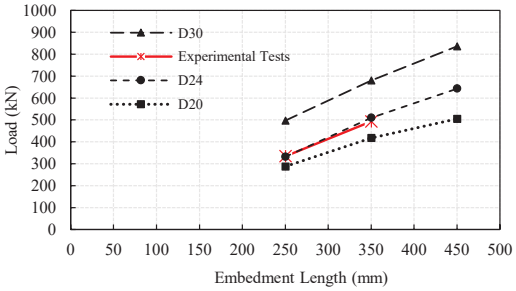

Figure 14. Numerical modeling and experimental test results of rods embedded parallel to the grain.

The pull-out strength of rods with 20- and 24-mm diameters embedded on the boundary of two cross-wised layers showed an increasing trend by increasing the rod diameter and embedment length. On the other hand, when the rod diameter was increased to 30 mm, they did not demonstrate a noticeably higher pull-out strength (as illustrated in Figure 15). This could be as a result of the rods being closer to the surface, which has been demonstrated to develop an early crack failure in experimental tests and numerical models.

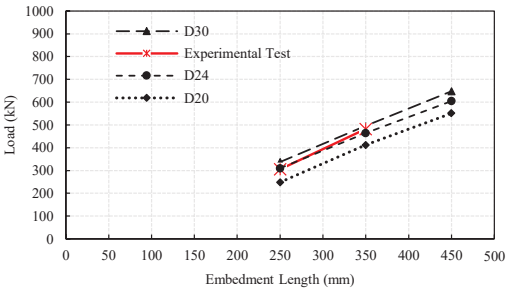

Figure 15. Numerical modeling and experimental test results of 5-layer CLT with rods embedded on the boundary of two cross-wised layers.

Using a new set of numerical models with a 7-layer CLT with rods on the boundary of two cross-wised layers, it was possible to overcome the stress distribution that reached the surface of CLTs, as illustrated in Figure 16. In this numerical model, the rod distance from the surface was extended to 84 mm while keeping the edge distance and rod distance at 84 mm and 72 mm, respectively. The interaction characteristics of this model were obtained from the characteristics of a 5-layer CLT with rods embedded on the boundary of two cross-wised layers.

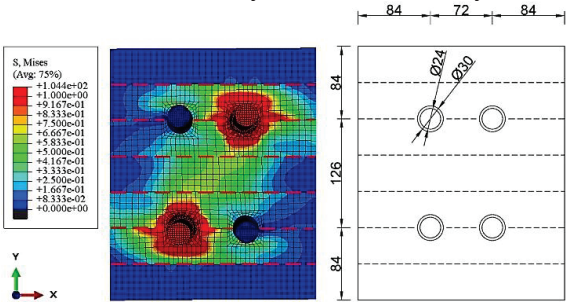

Figure 16. Numerical modeling of a 7-layer CLT containing rods embedded on the boundary of two cross-wised layers.

The numerical modeling of a 7-layer CLT with rods on the boundary of two cross-wised layers showed a proportional increase in the pull-out strength of rods with increasing the rod diameter and embedment length, as shown in Figure 17. By increasing the rod diameter from 24 to 30 mm when embedded on the boundary of two-cross-wised layers of a 5-layer CLT, the capacity of the connections increased by 9%, whereas for rods embedded on the boundary of a 7-layer CLT, the strength of the rods increased by 50%. The pull-out strength of rods with a diameter of 30 mm and embedment length of 450 mm was 738 kN. This occurrence demonstrated the negative impact of the rods' short surface distances for 5-layer CLTs. The pull-out strength of glued-in rods embedded

https://doi.org/10.52202/069179-0189

on the boundary of two cross-wised layers is lower compared to rods embedded perpendicular and parallel to the grain, even when the surface distance between the rods increased. This is because the surface cracking affected the rods' initial contact characteristics, and in practice, it is anticipated that the rods embedded on the boundary of two cross-wised layers of a 7-layer CLT to exhibit higher pull-out strength.

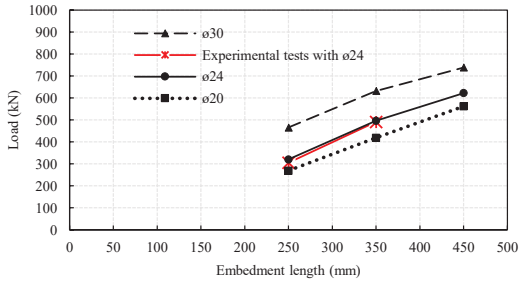

Figure 17. Numerical modeling and experimental test results of 7-layer CLT containing rods on the boundary of two-cross-wised layers.

4 CONCLUSIONS

High-capacity connections are required in designing high-rise buildings, and glued-in rods are one of the solutions to achieve this goal. Current full-scale monotonic and cyclic experimental tests are providing valuable results on the pull-out strength and seismic performance of CLT connections with multiple glued-in rods. The effect of the rods location regarding the laminations orientation is investigated, and stress distribution along the rods at various rod to lamination angles is provided.

According to the results of the experimental tests, the rod's failure mode and failure load were greatly influenced by the rod to lamination angle. Rods embedded perpendicular to the lamination led to the transverse layers rolling shear failure and crushed epoxy adhesive with a smooth force vs. displacement curve with maximum strength among tested configurations. If glued-in rods are used in CLT connections, it is recommended to embed them perpendicular to the grain. Due to the plug-out failure mode, rods embedded parallel to the grain demonstrated lower strength and a sharp strength reduction. Rods embedded on the boundary of two cross-wised layers demonstrated the lowest strength due to their closer distance to the surface of CLT, and rods containing epoxy adhesive were pulled out in a cylindrical shape. The results of the monotonic tests demonstrated that glued-in rod connections could only act ductile and fail when appropriately designed. Moreover, according to the cyclic loadings, glued-in rod connections maintain their elastic properties up until failure. The results of this investigation showed that glued-in rod connection technique could provide a solid connection for CLT construction. But it should be remembered that this investigation only looked at a certain kind of wood, adhesive, and rod. The increased list of parameters needs to be supplemented by more studies, such as using different glued-in rod connection details (rod sizes, adhesive types, spacings, and edge distance). In order to better understand the behaviour of glued-in rod connections, a wide range of test data with multiple failure mechanisms needs to be generated. Overall, this study demonstrated the high potential for this type of connection in CLT construction and showed that with glued-in rod connections, high capacities could be achieved.

ACKNOWLEDGEMENT

The first author wishes to express his gratitude to The University of Auckland for providing him with a Doctoral Scholarship to pursue his Ph.D. programme. The New Zealand Timber Design Society and WIDE Trust's financial help is also gratefully acknowledged.

REFERENCES

[1] Batchelar, M. L., & Mcintosh, K. A. (1998). Structural joints in glulam. In Proceedings of the 5th World conference in Timber Engineering, Montreux (pp. 17-20).

[2] Fragiacomo, M., Batchelar, M., Wallington, C., & Buchanan, A. (2010, June). Moment Joints in Timber Frames Using Glued-In Steel Rods: Experimental Investigation of Long-Term Performance. In World Conference on Timber Engineering, Riva del Garda, Trentino, Italy.

[3] Buchanan A. H.: Timber design guide. Third Edition. New Zealand Timber Industry Federation Inc., Wellington, New Zealand, 2007.

[4] Karacabeyli, E., & Douglas, B. (Eds.). (2013). CLT handbook: Cross-laminated timber. FPInnovations.

[5] Ayansola, G. S., Tannert, T., & Vallee, T. (2022). Experimental investigations of glued-in rod connections in CLT. Construction and Building Materials, 324, 126680.

[6] Azinović, B., Serrano, E., Kramar, M., & Pazlar, T. (2018). Experimental investigation of the axial strength of glued-in rods in cross laminated timber. Materials and Structures, 51(6), 1-16.

[7] European Committee for Standardization (CEN), EN 12512:2001, Timber Structures-Test Methods-Cycling Testing of Joints Made with Mechanical Fasteners, CEN, Brusells, 2001.

[8] Abaqus/CAE User's Manual, Version 6.23, USA, 2021.

[9] Muciaccia, G. (2019). An experimental approach to determine pull-out strength of single and multiple axially loaded steel rods bonded in glulam parallel to the grain. Wood Material Science & Engineering, 14(2), 88-98.

[10] Rossignon, A., & Espion, B. (2008). Experimental assessment of the pull-out strength of single rods bonded in glulam parallel to the grain. Holz als Roh- und Werkstoff, 66(6), 419-432.